Progress in Physics of Applied Materials 7 (2027), Serial Number 15, 31-36

Semnan University

Progress in Physics of Applied Materials

journal homepage: https://ppam.semnan.ac.ir/

Investigation of Transport Properties of Nanoribbons of γ-graphyne and graphdiyne by Tight-binding Model

M. Yeganeh [a], D. Vahedi Fakhrabad [b*]

[a] *School of Engineering, Kosar University of Bojnord, Bojnord, Iran*
[b] *Physics Department, Faculty of Science, University of Neyshabur, Neyshabur, Iran*

ARTICLE INFO

Article history:
Received: 10 May 2026
Revised: 29 July 2026
Accepted: 23 August 2026
Published online: 19 September 2026

Keywords:
Transport properties;
Tight-binding model;
γ-graphyne;
graphdiyne.

ABSTRACT

In this work, transport properties of nanoribbons of two carbon allotropes, including γ-graphyne and graphdiyne, were investigated using a tight-binding model in the non-equilibrium Green's function. We considered the carbon allotropes γ-graphyne, and graphdiyne, which respectively consist of 48 and 72 carbon atoms and are confined to semi-infinite leads of the same material. The electron transport coefficient showed an almost step-like quantized plateau for γ-graphyne, and graphdiyne reaching a transmission coefficient of up to 3 for both samples. The calculated band structure revealed the semiconducting behavior of γ-graphyne, and graphdiyne nanoribbons with band gap energies of 0.32 and 0.57 eV, respectively. The higher band gap of graphdiyne compared to γ-graphyne results in lower electronic conduction and thermal conductivity near the Fermi level; however, at chemical potentials further apart from the Fermi level which can be attained by gating or doping, higher electronic conduction and thermal conductivity in graphdiyne can be achieved compared to γ-graphyne.

1. Introduction

Natural and artificial allotropes of carbon with different hybridizations and dimensions have been of interest to scientists to investigate their properties and announce their potential applications [1]. Graphyne is an allotrope of layered carbon that was introduced in 1960 and then theoretically predicted in 1987 by Baughman et al. [2]. In this group of carbon allotropes, the presence of sp and sp2 hybridization of carbon atoms is observed in the two-dimensional (2D) plane [3]. The sp:sp2 ratio of carbon atoms, the number of intervening sp acetylenic linkage between two sp2 carbon atoms determine the type of graphyne, including α-, β-, γ-, 6, 6-12 graphyne, and graphdiyne structures [4, 5]. In resemblance to graphene, α-, β-, and 6, 6-12 graphyne have been revealed to exhibit semi-metallic behavior with a zero band gap. In contrast, based on the tight-binding model γ-graphyne, and graphdiyne have been shown to have band gap energies of 0.38, and 0.52 eV, respectively [4].

However, DFT calculations on γ-graphyne evaluated a bandgap of 0.47 eV [6], and 0.96 eV by utilizing hybrid functionals [7]. γ-graphyne belongs to the P6/mmm space group which presents stability against graphitization [8] and has lower thermal conductance and charge transport properties compared to graphene suggesting its suitability for the applications in semiconductor devices, electrode materials, lithium storage, ultraviolet light protectors, transistors, solar cell [9], and catalysts [1, 4, 10-12]. These characteristics have attracted the attention of researchers to further investigate these materials. Recent efforts toward the high-yield synthesis of γ-graphyne have been very encouraging in this area.

Therefore, it seems that this allotrope of carbon can show interesting function, and the necessity of further investigation of the γ-graphyne becomes more important.

* Corresponding authors.
E-mail addresses: davoud.vahedi@neyshabur.ac.ir

Cite this article as:

Yeganeh, M., Vahedi Fakhrabad, Investigation of Transport Properties of Nanoribbons of γ-graphyne and graphdiyne by Tight-binding Model. *Progress in Physics of Applied Materials*, *7*(2), pp.31-36.DOI: **10.22075/ppam.2026.41166.1227**

The semiconducting behavior of graphdiyne was also encouraging to study alongside γ-graphyne.

Since transport properties reflect the material and the characteristics of its surfaces and edges, here in this study we consider the carbon allotropes of γ-graphyne and graphdiyne- composed by 48 and 72 carbon atoms, respectively- connected to semi-infinite leads of the same material.

To the best of our knowledge the transport performance of graphdiyne by the tight-binding (TB) model has not yet been reported, however, the thermoelectric performance of γ-graphyne nanoribbon by introducing disordered surface fluctuation was investigated previously [13]. Therefore, in this work, the properties of two similar structures with armchair edge of γ-graphyne and graphdiyne were investigated using the TB model within the framework of the non-equilibrium Green's function (NEGF) formalism, and the results were discussed.

2. Computational Method

The study of the transport properties of the γ-graphyne and graphdiyne was carried out using the nearest-neighbor TB model within the framework of Green's function method [14]. The calculations were performed on a system comprises of three regions: a central scattering region including γ-graphyne or graphdiyne, and two semi-infinite left and right leads consisting of material similar to the scattering region. The Hamiltonian of the overall system can be written as:

$$H = \sum_i \varepsilon_i \, c_i^{\dagger} c_i - \sum_i (t_{i,i+1} c_i^{\dagger} c_{i+1} + h.c) \tag{1}$$

In which ε_i , $t_{i,i+1}$, and $c_i^{\dagger}$ (c_i) represent the energy of the *i*th site of the electron, the hopping energy between the nearest neighbor carbon atoms of γ-graphyne or graphdiyne, and the creation (annihilation) operator, respectively.

The on-site, and hopping energies in γ-graphyne are $\varepsilon_C = 0$, $t_1 = 2.75$, $t_2 = 3.11$, and $t_3 = 4.04$ eV [4]. The hopping parameters of t_1, t_2, and t_3 were schematically presented in Figure 1(b). The hopping energy variations between nearest neighbor C atoms are due to the presence of different *sp²-sp²*, *sp²-sp*, and *sp-sp* carbon bond. These tight binding parameters were calculated from the best fit of the tight binding results with DFT calculations on monolayer of γ-graphyne [15]. In a similar computational method, the tight binding parameters of graphdiyne were estimated by Sohrabi et al. as follows [4]: $\varepsilon_C = 0$, $t_1 = 3.46$ eV, $t_2 = 3.53$ eV, $t_3 = 4.04$ eV, $t_4 = 3.67$ eV.

The Hamiltonian matrix for the γ-graphyne system shown in Figure 1, is given by:

$$H = \begin{pmatrix} H_L & H_{L,M} & 0 \\ H_{L,M}^{\dagger} & H_M & H_{R,M}^{\dagger} \\ 0 & H_{R,M} & H_R \end{pmatrix} \tag{2}$$

$$H_{R,M} = \begin{pmatrix} H_{R,M}^{1,1} & H_{R,M}^{1,2} & \cdots & H_{R,M}^{1,48} \\ H_{R,M}^{21} & \ddots & \vdots & \vdots \\ \vdots & \cdots & \ddots & H_{R,M}^{47,48} \\ H_{R,M}^{48,1} & \cdots & H_{R,M}^{48,47} & H_{R,M}^{48,48} \end{pmatrix} \tag{3}$$

Where H_L, H_R, H_M, $H_{L,M}$, and $H_{R,M}$ denote the Hamiltonian matrices of the left lead, right lead, and scattering region, respectively. In the tight-binding representation, H_M is a sparse Hermitian matrix with zero on-site energies, while its nonzero off-diagonal matrix elements are given by the hopping parameters associated with the connected atomic sites. The matrices $H_{L,M}$, and $H_{R,M}$ represent the coupling between the scattering region and the left and right leads, respectively, and the superscript dagger (†) denotes the Hermitian conjugate. According to the interfacial bonding configuration of the γ-graphyne structure, the coupling matrix $H_{R,M}$ is highly sparse and contains only three non-zero elements, namely $H_{R,M}^{16,45}$, $H_{R,M}^{13,33}$, and $H_{R,M}^{4,32}$, while all other matrix elements are equal to zero. Similarly, the matrix $H_{L,M}$ also contains only three non-zero elements, located at the transposed positions $H_{R,M}^{45,16}$, $H_{R,M}^{33,13}$, and $H_{R,M}^{32,4}$, with all remaining entries being zero.

In accordance with Figure 1 and the bonding connections present in both structures, the coupling matrices $H_{L,M}$, and $H_{R,M}$ are sparse, each containing exactly three non-zero entries. This sparse form indicates that the electronic coupling is confined to the atomic sites directly connected at the interface between the scattering region and the corresponding leads.

The Green's function of the whole system is specified by:

$$G(E) = \left[EI - \hat{H}_M - \sum_L (E) - \sum_R (E)\right]^{-1} \tag{4}$$

Where I is the identity matrix, and $\sum_L(E)$ and $\sum_R(E)$ are the self-energy matrices that attain the coupling of the left and right leads to the scattering region. The transmission probability is defined as follows [16]:

$$T(E) = Tr\,[\Gamma_L G^r \Gamma_R G^a] \tag{5}$$

where G^r and G^arepresent the retarded and advanced Green's function of the system, and Γ_L and Γ_R are related to self-energies through $\sum_{L(R)} = -i/2\Gamma_{L(R)}$ and describe the linewidth coupling between the left and right lead to the γ-graphyne or graphdiyne

$$\sum_L (E) = H_{L,M}^{\dagger} G_L(E) H_{L,M} \tag{6}$$

$$\sum_R (E) = H_{R,M}^{\dagger} G_R(E) H_{R,M} \tag{7}$$

The $G_L(E) = (E - H_L)^{-1}$, and $G_R(E) = (E - H_R)^{-1}$ which are obtained by iteration method, are the surface Green's function for left and right leads. The surface Green's

function in defined semi-infinite leads will not change and can be calculated as [17]:

$$G_{L(R)}(E) = (E - H_0 - H_1 G_{L(R)} H_1^{\dagger})^{-1} \quad (8)$$

where the H_0 and H_1 are the Hamiltonians of the added layer and the coupling between the nearest layers.

(a)

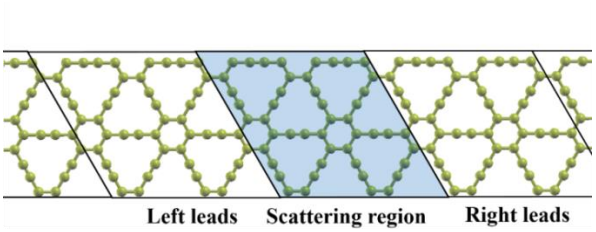

(b)

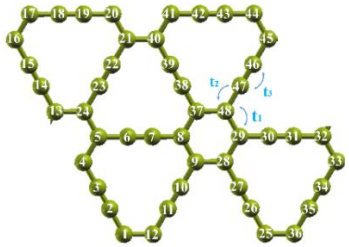

(c)

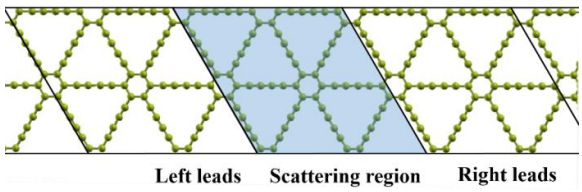

(d)

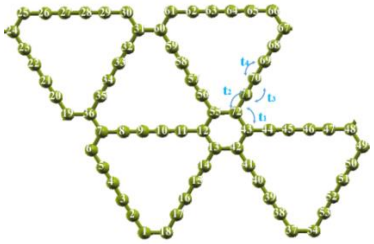

Fig. 1: Schematic illustration of the transport setup and atomic structures of γ-graphyne and graphdiyne. (a,b) Corresponding γ-graphyne structure and its atom-numbering scheme, with the relevant hopping parameters indicated. Left lead, scattering region, and right lead used in the transport calculations, with the scattering region highlighted by the shaded area. (c,d) Corresponding graphdiyne structure and its atom-numbering scheme, with the hopping parameters marked by blue arrows.

The density of states is defined by the following relationship:

$$DOS(E) = -\frac{1}{\pi} Im[Tr(G(E))] \quad (9)$$

The transport coefficient $L_n(\mu, T)$ when $\mu_L = \mu_R$, is as following [18, 19]:

$$L_n(\mu, T) = \frac{1}{h} \int T(E)(E - \mu)^n \left[-\frac{\partial f_{\mu,T}}{\partial E} \right]_{\mu,T} dE \quad (10)$$

In which $\frac{\partial f}{\partial E} = \frac{1}{4K_B T} [\cosh(\frac{E-E_F}{2K_B T})]^{-2}$ is the thermal broadening function.

Then electronic conductance, and electronic thermal conductivity can be obtained by the subsequent equations [20]:

$$G_e = e^2 L_0 \quad (11)$$

$$k_e = \frac{1}{T} \left(L_2 - \frac{L_1^2}{L_0} \right) \quad (12)$$

3. Results and Discussion

Two-probe devices made of γ-graphyne or graphdiyne with armchair edges including a central scattering region connected to semi-infinite right and left electrodes composed of γ-graphyne or graphdiyne, respectively were presented in Figure 1 (a-d). The central region of γ-graphyne contains of 48 carbon atoms (Figure 1b) while that of graphdiyne contains 72 carbon atoms (Figure 1d). As shown in Figure 1 (1(a) and 1(c)), the widths of the right and left leads at the contact points with scattering region are similar to the width of scattering region itself, which is approximately 13.78 Å for γ-graphyne and 18.9 Å for graphdiyne. An attempt has been made to select a shape similar to γ-graphyne and graphdiyne in terms of the number of hexagonal rings. However, since the number of carbon atoms and the number of sp acetylenic linkage in hexagonal rings of γ-graphyne and graphdiyne are different, the total number of atoms in the scattering region in these two structures is different. However, the number of transmission channels in the studied γ-graphyne and graphdiyne is similar.

The band structure of γ-graphyne and graphdiyne was illustrated in Figure 2 indicating the semiconducting nature of these structures with band gaps of about 0.32 and 0.57 eV, respectively. The results are consistent with the reported band gaps of 0.38, and 0.46 eV for γ-graphyne and 0.48 (GGA-PBE), and 0.52 eV for graphdiyne [4, 21, 22]. The local density of states (LDOS) of γ-graphyne and graphdiyne, presented in Figure 3a, also reveals their semiconducting behaviors and can give a deeper insight into the transmission curve as illustrated in Figure 3b. The observed band gaps in the band structure or density of states result in low electron transmission or electrical conductivity at or near the Fermi energy level (EF). However, at the energies where the density of states spectrum enhances, the transmission curve also increases, denoting that the electrons can be conducted more efficiently in these ribbons.

The transmission curve shows a symmetric pattern around Fermi energy which was set to zero (E_F=0) and demonstrates the electron-hole symmetry of the Hamiltonian. Every sub-band of the band structure shows transmission of one in ideal ballistic transport, and at a

given electron energy, transmission is calculated by the transmission probability multiply by the number of transport channels. In perfect structures with no scattering, the transmission probability is equal to 1; therefore, the number of transport channels specify the magnitude of transmission. The electron transmission coefficient shows a nearly step-shaped quantized plateau for γ-graphyne and graphdiyne reaching a maximum of 3 indicating the number of transmission channels for electron transport from one lead to another. The enhancement or reduction of the transmission above and below Fermi energy of the γ-graphyne or graphdiyne follows the LDOS pattern.

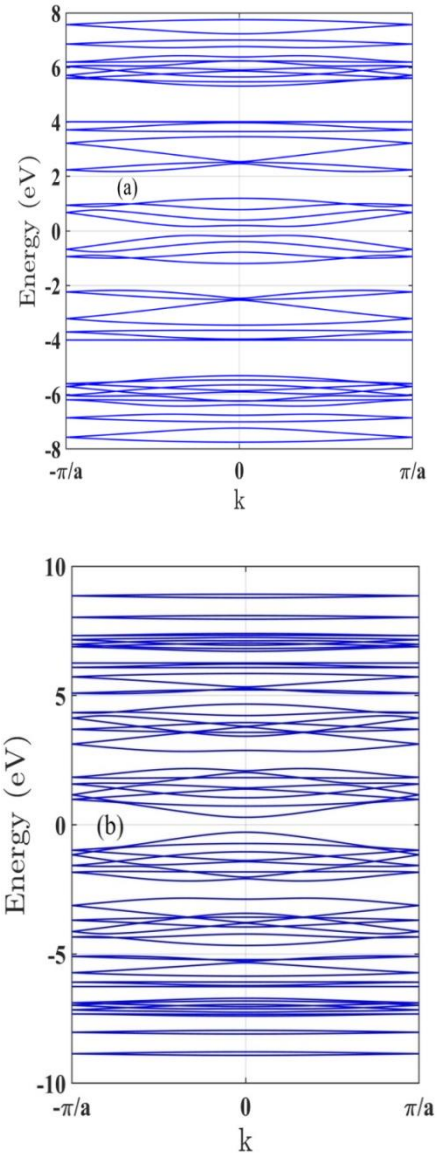

Fig. 2: Band structure of (a) γ-graphyne and (b) graphdiyne.

The room temperature electronic conductance (G_e), and electronic thermal conductivity (k_e) of the nanoribbons in terms of chemical potential (μ) were presented in Figure 4. It can be seen that similar to the electronic transmission coefficient, the electronic conductance confirms the higher bandgap of graphdiyne compared to γ-graphyne. In the Fermi energy range (-1 to 1 eV), γ-graphyne exhibits higher conductance than graphdiyne due to the latter's larger bandgap; however, at energies above this range, graphdiyne demonstrates higher conductivity and a pattern characterized by more intense oscillations compared to γ-graphyne.

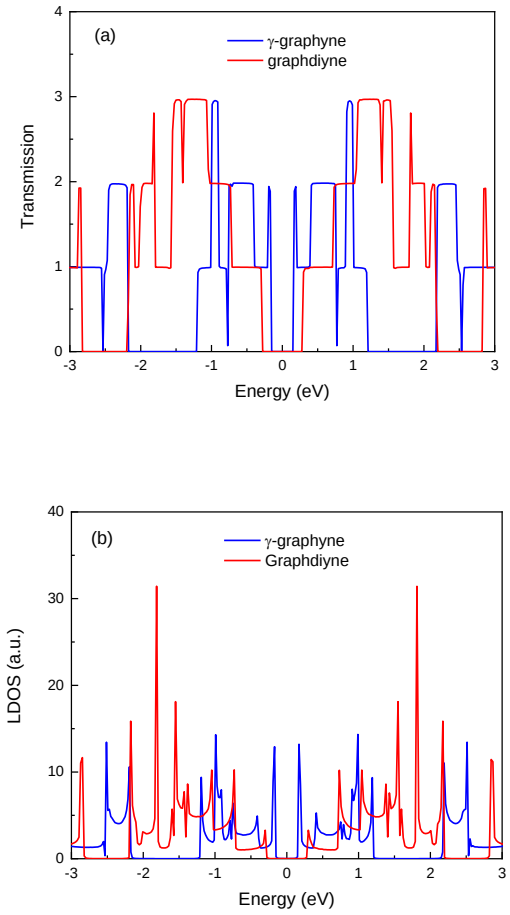

Fig. 3: (a) Transmission of the γ-graphyne and graphdiyne and (b) the LDOS of the transmission.

Both G_e and k_e depend on the transmission coefficient according to equations (11) and (12) and present similar patterns of enhancement and suppression to transport coefficient. The chemical potential of γ-graphyne and graphdiyne can be tuned with gating or doping. Although, the higher band gap of graphdiyne compared to γ-graphyne leads to lower electronic conduction and thermal conductivity near the Fermi level, at higher chemical potential that can be achieved by gating or doping, higher electronic conduction and thermal conductivity can be attained in graphdiyne compared to γ-graphyne. Also, since the density of states of graphdiyne is greater at higher energies, electrons with these energies can provide higher electronic conduction and thermal conductivity in graphdiyne compared to γ-graphyne [23].

The maximum electronic thermal conductivity for γ-graphyne and graphdiyne is 1110 pW/K at energies of ± 0.58 eV and 1667 pW/K at energies of ± 1.24 eV, respectively. Zhou et al. [13] estimated the electronic thermal conductivity of γ-graphyne (with a length and width of about 13.72 and 1.45 nm) to be about 1647 pW/K at energies of ± 0.75 eV, which is slightly higher than the value calculated in this work. In their work, disordered surface fluctuation was applied to the

nanoribbon of γ-graphyne with the aim of enhancing thermoelectric performance. It has been shown that the ribbon length affects phonon scattering, leading to lower thermal conductance and consequently higher thermoelectric performance. Conversely, as width of the nanoribbon increases, the thermoelectric efficiency decreases. The central scattering region in this work has fewer electron transport channels compared to central region of their choice; therefore, the lower electron transport channels can reduce the transmission as well as the conduction compared to their work [13].

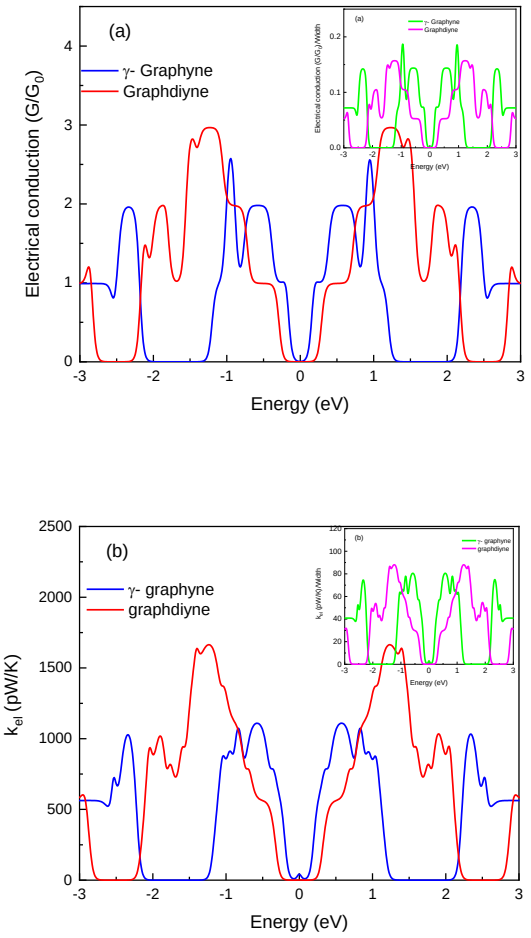

Fig. 4: (a) Electronic conductivity ($G_0=2e^2/h$), and (b) electronic contribution to thermal conductivity. The insets show the conductivity divided by the length of the scattering region in contact to the leads.

The Overall results in this work show the higher transport properties of graphdiyne compared to γ-graphyne. In order to infer the effects of width (number of atoms in hexagonal rings) on electronic conductance, and electronic thermal conductivity, Figure 4(a) and 4(b) were normalized by the width of scattering region at the contact points with the leads and the results were presented in the inset of these figures. In the insets, the conductivity difference between γ-graphyne and graphdiyne is almost eliminated, indicating a positive effect of increasing the width or the number of atoms on the conductivity.

4. Conclusion

The transport properties of γ-graphyne and graphdiyne were investigated by tight-binding model in the non-equilibrium Green's function. The calculations indicated that γ-graphyne and graphdiyne have semiconducting behavior having band gaps of 0.32 and 0.57 eV, respectively. The calculation of the electronic part of the transport properties of γ-graphyne and graphdiyne revealed the higher conductance and thermal conductivity of graphdiyne in comparison to γ-graphyne.

Funding Statement

This research received no specific grant from any funding agency.

Conflicts of Interest

The authors declare no conflicts of interest.

Authors Contribution Statement

Mahboubeh Yeganeh: Writing – original draft, Writing – review & editing, Investigation, Validation, Formal analysis and interpretation, Visualization.

Davoud Vahedi Fakhrabad: Computational Methodology, Data validation, Visualization, Formal analysis and interpretation, Writing – review & editing

References

[1] Barua, M., Saraswat, A., & Rao, C.N.R. 2017. A novel method for synthesis of γ-graphyne and their charge transfer properties. *Carbon*, 200, pp.247-252.

[2] Baughman, R.H., Eckhardt, H., & Kertesz, M. 1987. Structure-property predictions for new planar forms of carbon: Layered phases containing sp2 and sp atoms. *The Journal of Chemical Physics*, 87(11), pp.6687-6699.

[3] Ivanovskii, A.L. 2013. Graphynes and graphdyines. *Progress in Solid State Chemistry*, 41(1-2), pp.1-19.

[4] Sani, S.S., Mousavi, H., Asshabi, M., & Jalilvand, S. 2020. Electronic properties of graphyne and graphdiyne in tight-binding model. *ECS Journal of Solid State Science and Technology*, 9(3), p.031003.

[5] Coluci, V.R., Braga, S.F., Legoas, S.B., Galvao, D.S., & Baughman, R.H. 2003. Families of carbon nanotubes: Graphyne-based nanotubes. *Physical Review B*, 68(3), p.035430.

[6] Ashhadi, M. 2017. Electronic transport properties and first-principles study of γ-graphyne, and γ-BN graphyne monolayers. *Superlattices and Microstructures*, 111, pp.1162-1171.

[7] Guo, Y., Jiang, K., Xu, B., Xia, Y., Yin, J., & Liu, Z. 2012. Remarkable hydrogen storage capacity in Li-decorated graphyne: theoretical predication. *The Journal of Physical Chemistry C*, 116(26), pp.13837-13841.

[8] Ouyang, T., Cui, C., Shi, X., He, C., Li, J., Zhang, C., ... & Zhong, J. 2020. Systematic Enumeration of Low-Energy Graphyne Allotropes Based on a Coordination-Constrained Searching Strategy. *Physica Status Solidi (RRL)–Rapid Research Letters*, 14(12), p.2000437.

[9] Shi, Z., Khaledialidusti, R., Malaki, M., & Zhang, H. 2021. MXene-based materials for solar cell applications. *Nanomaterials*, 11(12), p.3170.

[10] Ming, S., Qin, L., Wang, S., Zhang, C., Hou, C., Zhang, Y., ... & Hou, H. 2024. 4-6 carbophene: A two-dimensional carbon material with Dirac cone and superior activity for electrochemical oxygen reduction reactions. *Diamond and Related Materials*, 141, p.110603.

[11] Liu, Q., Wang, X., Yu, J., & Wang, J. 2024. Graphyne and graphdiyne nanoribbons: from their structures and properties to potential applications. *Physical Chemistry Chemical Physics*, 26(3), pp.1541-1563.

[12] Rana, S., Kumar, A., Dhiman, P., Sharma, G., Amirian, J., & Stadler, F.J. 2024. Progress in graphdiyne and phosphorene based composites and heterostructures as new age materials for photocatalytic hydrogen evolution. *Fuel*, 356, p.129630.

[13] Zhou, B., Zhou, B., & Zhou, G. 2019. Optimizing the thermoelectric performance of γ-graphyne nanoribbons via introducing disordered surface fluctuation. *Solid State Communications*, 298, p.113646.

[14] Paxton, A.T. 2009. An introduction to the tight binding approximation–implementation by diagonalisation. *NIC Series*, 42, pp.145-176.

[15] Ashhadi, M. 2017. Electronic transport properties and first-principles study of γ-graphyne, and γ-BN graphyne monolayers. *Superlattices and Microstructures*, 111, pp.1162-1171.

[16] Maiti, S.K. 2007. Quantum transport through polycyclic hydrocarbon molecules. *Physics Letters A*, 366(1-2), pp.114-119.

[17] Bazrafshan, M.A., & Khoeini, F. 2024. Flexible thermoelectrics in crossed graphene/hBN composites. *Scientific Reports*, 14(1), p.1079.

[18] Karamitaheri, H. 2013. Thermal and thermoelectric properties of nanostructures (Doctoral dissertation, Technische Universität Wien).

[19] Kalami, R., & Ketabi, S.A. 2021. Spin-dependent thermoelectric properties of a magnetized zigzag graphene nanoribbon. *Progress in Physics of Applied Materials*, 1(1), pp.1-6.

[20] Ajeel, F.N., & Ahmed, A.B. 2023. Tuning the thermoelectric properties of graphene nanoribbons by vacancy defect with Ge-doping. *Chemical Physics Impact*, 7, p.100367.

[21] Wang, X.M., Mo, D.C., & Lu, S.S. 2013. On the thermoelectric transport properties of graphyne by the first-principles method. *The Journal of Chemical Physics*, 138(20).

[22] Sun, L., Jiang, P.H., Liu, H.J., Fan, D.D., Liang, J.H., Wei, J., ... & Shi, R. 2015. Graphdiyne: A two-dimensional thermoelectric material with high figure of merit. *Carbon*, 90, pp.255-259.

[23] Kalami, R., & Ketabi, S.A. 2025. Exploring the electronic and thermoelectric properties of zigzag and armchair edge Irida-Graphene nanoribbons. *Journal of Computational Electronics*, 24(1), p.22.